Efficient mid-IR spectral generation via spontaneous fifth-order cascaded-Raman amplification in silica fibers

Peter T. Rakich,* Yoel Fink, and Marin Soljačić

Research Laboratory of Electronics, Massachusetts Institute of Technology, 77 Massachusetts Avenue, Cambridge, Massachusetts 02139, USA

**Corresponding author: rakich@alum.mit.edu*

Received April 2, 2008; revised June 9, 2008; accepted June 10, 2008; posted June 13, 2008 (Doc. ID 94589); published July 24, 2008

Spontaneous cascaded Raman amplification is demonstrated as a practical and efficient means of power transfer from telecommunications wavelengths to mid-IR wavelength bands through use of conventional silica fibers and amplifiers. We show that silica fibers possessing normal dispersion over all near-IR and mid-IR wavelengths can facilitate 37% and 16% efficient Raman power conversion from 1.53 μm to 2.15 and 2.41 μm wavelength bands, respectively, using nanosecond pulses from an all-fiber laser source. In contrast to supercontinuum-based techniques for long-wavelength generation, the high levels of Raman gain generated at these wavelength bands could produce useful optical amplification necessary for the development of numerous mid-IR laser sources.

OCIS codes: 140.3550, 140.3538, 190.5650, 190.5890, 140.4480.

Light sources spanning mid-IR wavelengths are the subject of intense interest for such applications as semiconductor processing, coherent x-ray generation, chemical sensing, and cancer detection [1]. To this end, sources spanning mid-IR wavelengths have been developed in the form of quantum-cascade lasers [2], rare-earth-doped fiber-gain media [3], and fiber-based supercontinuum sources [4]. In this Letter, we present a simple and practical means of generating mid-IR wavelengths through spontaneous cascaded-Raman (CR) amplification, demonstrating efficient and controlled spectral transfer from telecommunications wavelengths to mid-IR wavelength bands through spontaneously seeded Raman amplification in normal dispersion silica fibers. Through use of a low-noise all-fiber nanosecond pulsed source employing erbium amplifiers, as much as 37% (16%) of the incident pump light (centered at 1.53 μm) is transfered to 2.14 (2.41) μm wavelength bands.

It has been demonstrated that at high powers, substantial levels of Raman gain can be achieved through the use of conventional silica fibers to produce significant spectral redshifts through spontaneous CR processes [5–8]. Knowing this, the possibility of constructing simple and efficient Raman-based sources and gain blocks for long-wavelength spectral generation seems promising. However, one's ability to continually redshift through CR does suffer some practical limitations. Spectral broadening and pulse distortions owing to both spontaneous Raman emission and four-wave mixing (FWM) generally limit the efficiency of this process.

For instance, at high powers, anomalous dispersion and Kerr nonlinearities can give rise to modulation instabilities, yielding significant spectral broadening and pulse distortion and unnecessarily stifling the efficiency of the CR process. For this reason, normal dispersion fibers are more desirable for controlled and maximally efficient CR at the nanosecond time scale.

Unfortunately, silica fibers generally possess anomalous dispersion from 1.3 to 2.4 μm owing to the presence of a strong mid-IR absorption resonance [9]. However, we illustrate that normal fiber dispersion can be obtained over the entire silica transparency window through proper choice of fiber cutoff wavelength (λ_c) and NA. Since the waveguide dispersion of a step-index fiber is normal (in sign), and monotonically increasing in magnitude for wavelengths λ_c to $2.2\lambda_c$, the waveguide dispersion can be made to match the material dispersion for sufficiently high NA, making the total chromatic dispersion of the fiber normal for all wavelengths [10]. This can be seen in Fig. 1(b), which shows the regions of normal and anomalous dispersion for a silica step-index fiber with a cutoff wavelength of 1.45 μm. For an NA of greater than 0.4, the zero-dispersion wavelength is pushed to 2.6 μm, enabling normal dispersion for the entire transparency window of silica.

In what follows, we examine spontaneous Raman amplification using a germanium-doped (~58 wt.% Ge doping) step-index fiber (Nufern UHNA7) with a λ_c of 1.45 μm and an NA of 0.41. The computed dispersion and measured loss profiles for this fiber can be seen in Figs. 1(b) and 1(c), showing normal dispersion over the entire transparency window of the fiber. Note that although the dispersive effects of dopants are not included in the computations of Fig. 1(a), high doping concentrations can result in nonnegligible redshifts of zero of dispersion wavelength of silica (i.e., up to 3%).

Maximally efficient spontaneous Raman transfer requires a spectrally narrow laser source, with a low amplified spontaneous emission (ASE) pedestal, since the extent of FWM-induced spectral broadening is generally very sensitive to initial conditions. To this end, we developed the fiber-based laser source seen in Fig. 2(a), which produces 2 ns pulses at a variable repetition rate, making output powers of several kilowatts possible [4,11]. The source amplifies

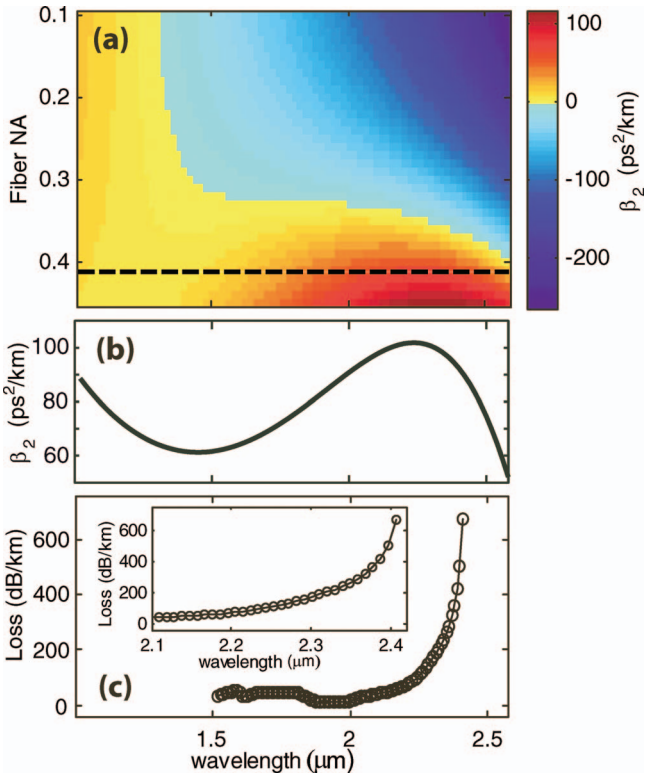

Fig. 1. (a) Dispersion versus NA and wavelength for a silica fiber (λ_c=1.45 μm). (b) Computed dispersion and (c) measured loss for NUFERN UHNA7 silica fiber.

seed pulses from an electrically gain-modulated distributed-feedback (DFB) laser diode through two stages of erbium gain. In the first stage, the seed pulses of 1531.12 nm wavelength are copropagated with a cw seed signal from a tunable laser source (detuned from the DFB wavelength by ~100 GHz). The cw signal produces saturation of the amplifiers, ensuring a very low ASE component to the amplified seed signal. Once the seed pulses reach 10 mW average power levels, a fiber Bragg grating with a 10-GHz-wide stopband is used, in conjunction with a circulator, to spectrally filter the seed pulses from the amplified cw laserline and ASE background signals. With sufficient power to saturate the second stage of erbium gain, the pulses are boosted to average powers of 240 mW, yielding an ASE component that is typically less than 1% of the total output power.

To produce spontaneous Raman energy transfer, the output of the high-power amplifier is spliced to 50 m of small-core normal-dispersion silica fibers (Nufern UHNA7). It should be noted that splice losses (0.5 dB) and linear propagation losses (1.5 dB) reduce the laser output power from 240 to 150 mW at 1.53 μm wavelengths. For a repetition rate of 680 kHz, the laser output is measured with spectrometer and PbSe detector as a function of laser power. The spectral evolution of the resulting cascaded Raman process is summarized by the intensity map of Fig. 3(a) as the laser power is increased, showing significant and controlled spectral redshifts through higher-order CR power transfer. As the laser power is increased we see that the fundamental (1531 nms) pump wavelength is shifted in 14.7 THz (or 490 cm^{-1}) steps [8,12] to 1.64, 1.78, 1.94, 2.14, and 2.41 μm wavelength bands. While the spectral width of each successive order does broaden, the generated spectral bands are very clean, showing negligible power shedding to continuum. Despite the high material losses of silica at 2.41 μm, a strong fifth Raman order is formed, producing significant power transfer.

The efficiency of power transfer to long wavelengths can be more precisely examined by integration of the laser power measured in each Raman order as the average laser power is increased. The measured fraction of laser power found in each order

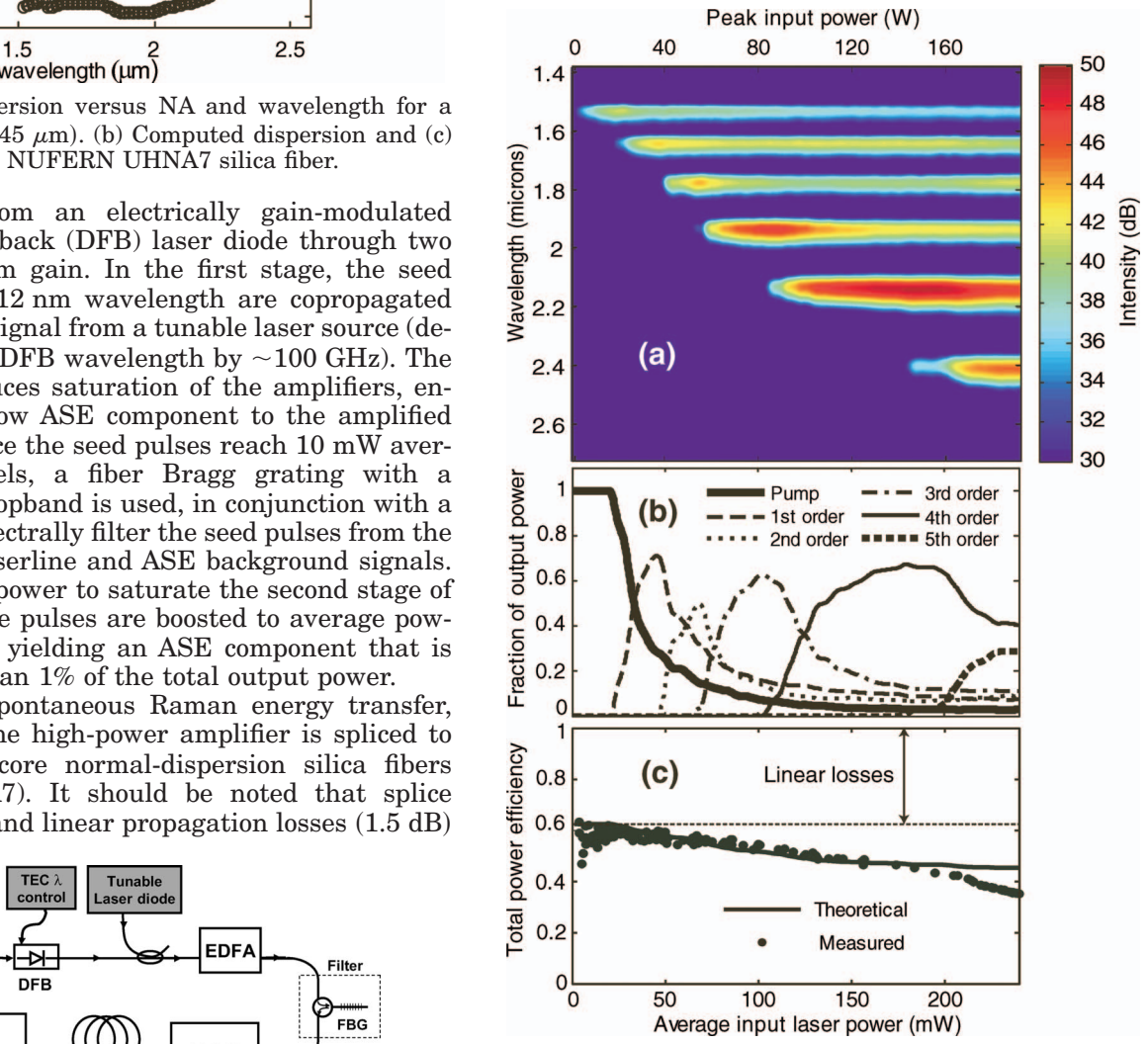

Fig. 3. (a) Measured spectral intensity versus wavelength (μm) and laser power. (b) Fraction of laser power in each order versus incident laser power. (c) Measured (circles) and estimated (solid curve) total power efficiency.

Fig. 2. Schematic of fiber-based pulsed laser source.

can be seen in Fig. 3(b), revealing that as much as 68% of the output power is transferred to the 2.14 μm wavelengths, while 30% is transferred to 2.41 μm wavelengths. Accounting for the splice and propagation losses of the fiber, we see that these percentages correspond to 37% and 16% total power conversion efficiencies to 2.14 μm and 2.41 μm wavelength bands, respectively. Remarkably, at maximum output power, less than 2% of the incident laser power remains at 1.53 μm.

As seen in Fig. 3(c), the total power efficiency of the Raman conversion process was directly obtained by measuring the power exiting the fiber with a thermal power meter. For increasing spectral redshifts (or increasing powers) one finds that the total power efficiency monotonically decreases from 62% (consistent with linear losses) to 35%, indicating that nonlinearly induced power dissipation occurs at higher powers. Note that some component of the losses is a fundamental consequence of the Raman process, which requires that each Stokes-shifted photon coincides with the production of a (dissipative) phonon. An estimate of the power efficiency attributable to Raman process (or phonon-induced losses) can be made using the known quantum efficiency of the Raman process and the measured power fraction in each Raman order, as is shown by a solid curve in Fig. 3(c), revealing reasonable agreement with measurement. The discrepancy between the estimated and measured efficiencies is most pronounced at high powers, indicating that high silica absorption losses at 2.41 μm wavelengths are limiting the efficiency of the power transfer at long wavelengths.

Finally, we examine the temporal evolution of the laser pulse through the spontaneous Raman process. The measured initial pulse profile (before entering the nonlinear fiber) is seen in Fig. 4(a), while the pulse profiles found by spectrally resolving the pump (solid curve) and first Raman order (dashed curve) exiting the nonlinear fiber can be seen in Fig. 4(b), revealing that the central portion of the pulse is transferred from 1.53 to 1.64 μm, leaving only the wings of the pulse behind. Pulse apodization of this form is well understood in the context of spontaneous Raman buildup [5,6] and results from the intensity dependence of the Raman gain. These measurements agree well with temporal simulations, found through coupled amplitude equations incorporating dispersion, Kerr nonlinearities, and Raman terms [8], seen in Figs. 4(c) and 4(d). Interestingly, the peak pulse intensity and pulse shape are essentially preserved, allowing the same process to occur numerous times. Finally, we note that the walk-off length for the pump and Stokes wavelengths is ~300 m for 2 ns pulse durations, meaning that dispersion has little impact on the temporal evolution at these length scales.

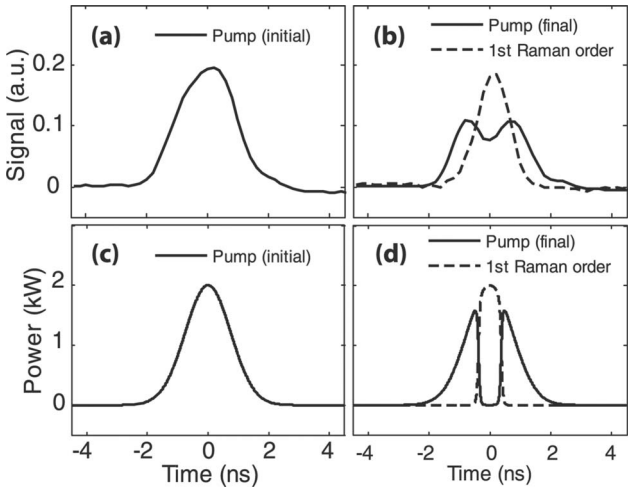

Fig. 4. (a) and (b) Measured pulse profiles. (c) and (d) Simulated pulse profiles for comparison.

In conclusion, we have shown that, through use of silica fibers possessing normal dispersion over near-IR and mid-IR wavelengths, 37% (16%) efficient Raman power transfer from 1.53 μm to 2.15 (2.41) μm wavelength bands can be obtained using nanosecond pulses from an all-fiber laser source. In this case, the total conversion efficiencies were unnecessarily limited by fiber losses. However, efficiencies approaching 70% can, in principle, be achieved at these wavelengths if fiber losses are made negligible. Finally, in contrast to supercontinuum techniques for long-wavelength generation, we note that high levels of Raman gain generated at these wavelength bands could produce useful optical amplification necessary for the development of numerous mid-IR laser sources.

We thank E. P. Ippen and J. W. Sickler for helpful discussions. This work was supported by the Air Force Research Laboratories (grant FA8650-05-C-5426) and the Army Research Office via The Institute for Soldier Nanotechnologies (contract W911NF-07-D-0004).

References

1. J. S. Sanghera, I. D. Aggarwal, L. B. Shaw, L. E. Busse, P. Thielen, V. Nguyen, P. Pureza, S. Bayya, and F. Kung, J. Optoelectron. Adv. Mater. **3**, 627 (2001).
2. P. Werlea, F. Slemra, K. Maurera, R. Kormannb, R. Mucke, and B. Janker, Appl. Phys. B **67**, 307 (1998).
3. L. Esterowitz, R. Allen, and I. Aggarwal, Electron. Lett. **24**, 1104 (1988).
4. C. A. Xia, M. Kumar, O. R. Kulkarni, M. N. Islam, F. L. Terry, and M. J. Freeman, Opt. Lett. **31**, 2553 (2006).
5. R. H. Stolen, C. Lee, and R. K. Jain, J. Opt. Soc. Am. B **1**, 652 (1984).
6. C. Lin, L. G. Cohen, R. H. Stolen, G. W. Tasker, and W. G. French, Opt. Commun. **20**, 426 (1977).
7. S. V. Chernikov, Y. Zhu, J. R. Taylor, and V. P. Gapontsev, Opt. Lett. **22**, 298 (1997).
8. G. P. Agrawal, *Nonlinear Fiber Optics* (Academic, 1989), Chap. 8.
9. H. Xie, Z. C. Wang, and J. X. Fang, Phys. Status Solidi A **96**, 483 (1986).
10. K. Okamoto, *Fundamentals of Optical Waveguides* (Academic, 2000).
11. O. P. Kulkarni, C. Xia, D. J. Lee, M. Kumar, A. Kuditcher, M. N. Islam, F. L. Terry, M. J. Freeman, B. G. Aitken, S. C. Currie, J. E. McCarthy, M. L. Powley, and D. A. Nolan, Opt. Express **14**, 7924 (2006).
12. R. H. Stolen, C. Lee, and R. K. Jain, J. Opt. Soc. Am. B **1**, 652 (1984).